Figure S1

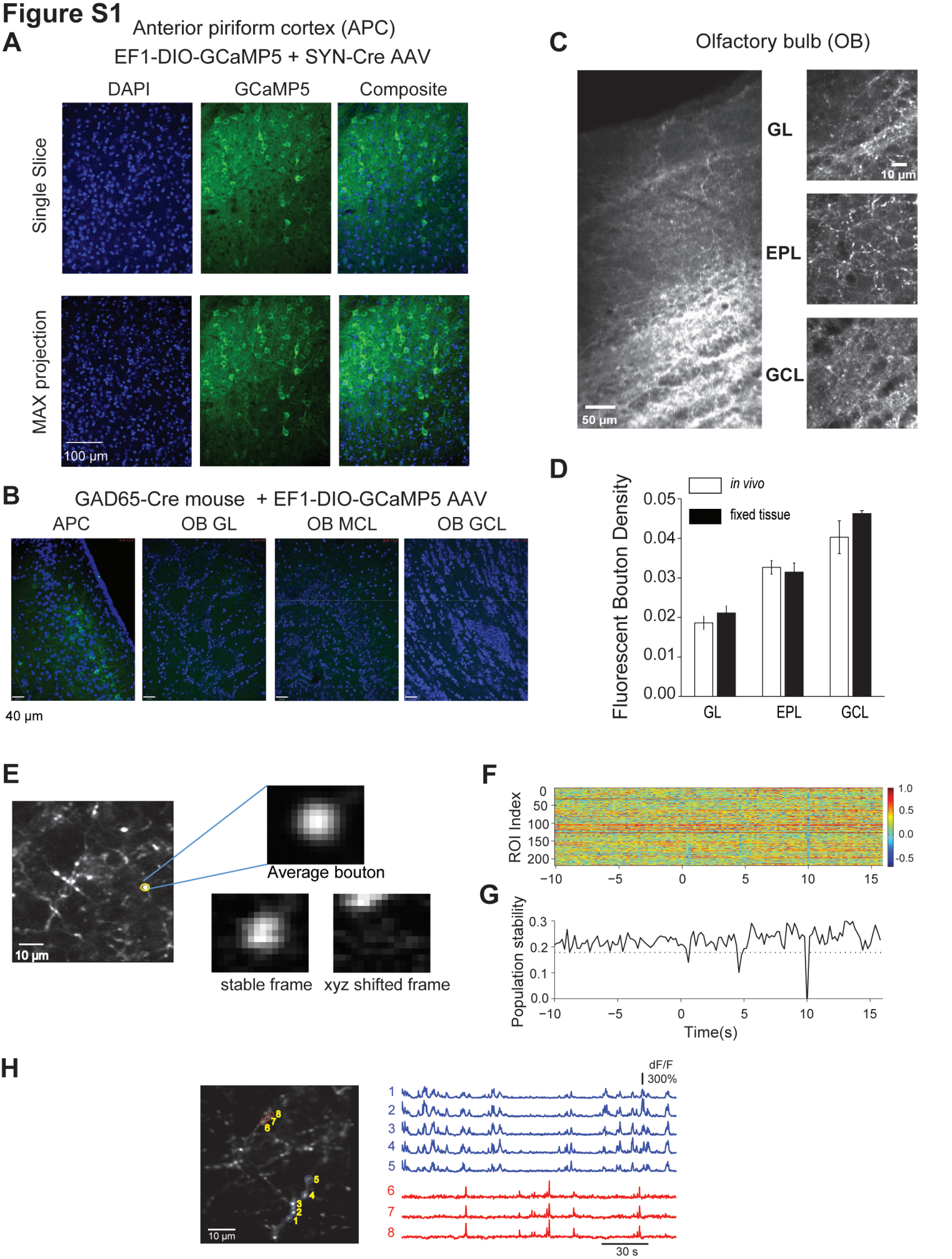
A
Anterior piriform cortex (APC)
EF1-DIO-GCaMP5 + SYN-Cre AAV
DAPI
GCaMP5
Composite
Single Slice
MAX projection
100 µm
B
GAD65-Cre mouse + EF1-DIO-GCaMP5 AAV
APC
OB GL
OB MCL
OB GCL
40 µm
C
Olfactory bulb (OB)
GL
EPL
GCL
50 µm
10 µm
D
Fluorescent Bouton Density
in vivo
fixed tissue
0.05
0.04
0.03
0.02
0.01
0.00
GL
EPL
GCL
E
10 µm
Average bouton
stable frame
xyz shifted frame
F
ROI Index
0
50
100
150
200
−10
−5
0
5
10
15
1.0
0.5
0.0
-0.5
G
Population stability
0.3
0.2
0.1
0.0
−10
−5
0
5
10
15
Time(s)
H
10 µm
dF/F
300%
1
2
3
4
5
6
7
8
30 s

Figure S2

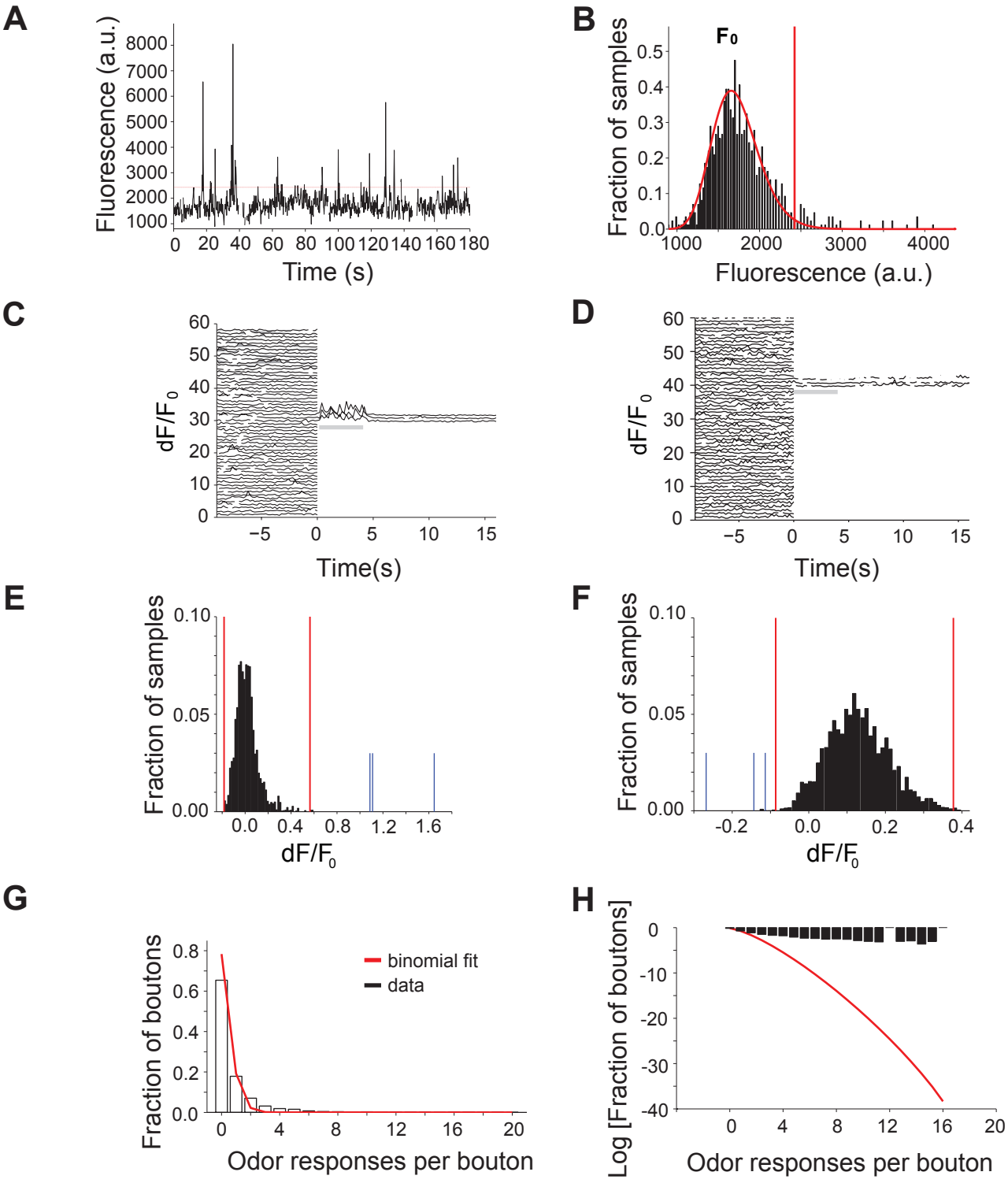
A
Fluorescence (a.u.)
8000
7000
6000
5000
4000
3000
2000
1000
0 20 40 60 80 100 120 140 160 180
Time (s)
B
F0
Fraction of samples
0.5
0.4
0.3
0.2
0.1
0.0
1000 2000 3000 4000
Fluorescence (a.u.)
C
dF/F0
60
50
40
30
20
10
0
−5 0 5 10 15
Time(s)
D
dF/F0
60
50
40
30
20
10
0
−5 0 5 10 15
Time(s)
E
Fraction of samples
0.10
0.05
0.00
0.0 0.4 0.8 1.2 1.6
dF/F0
F
Fraction of samples
0.10
0.05
0.00
-0.2 0.0 0.2 0.4
dF/F0
G
Fraction of boutons
0.8
0.6
0.4
0.2
0.0
0 4 8 12 16 20
Odor responses per bouton
binomial fit
data
H
Log [Fraction of boutons]
0
-10
-20
-30
-40
0 4 8 12 16 20
Odor responses per bouton

Figure S3

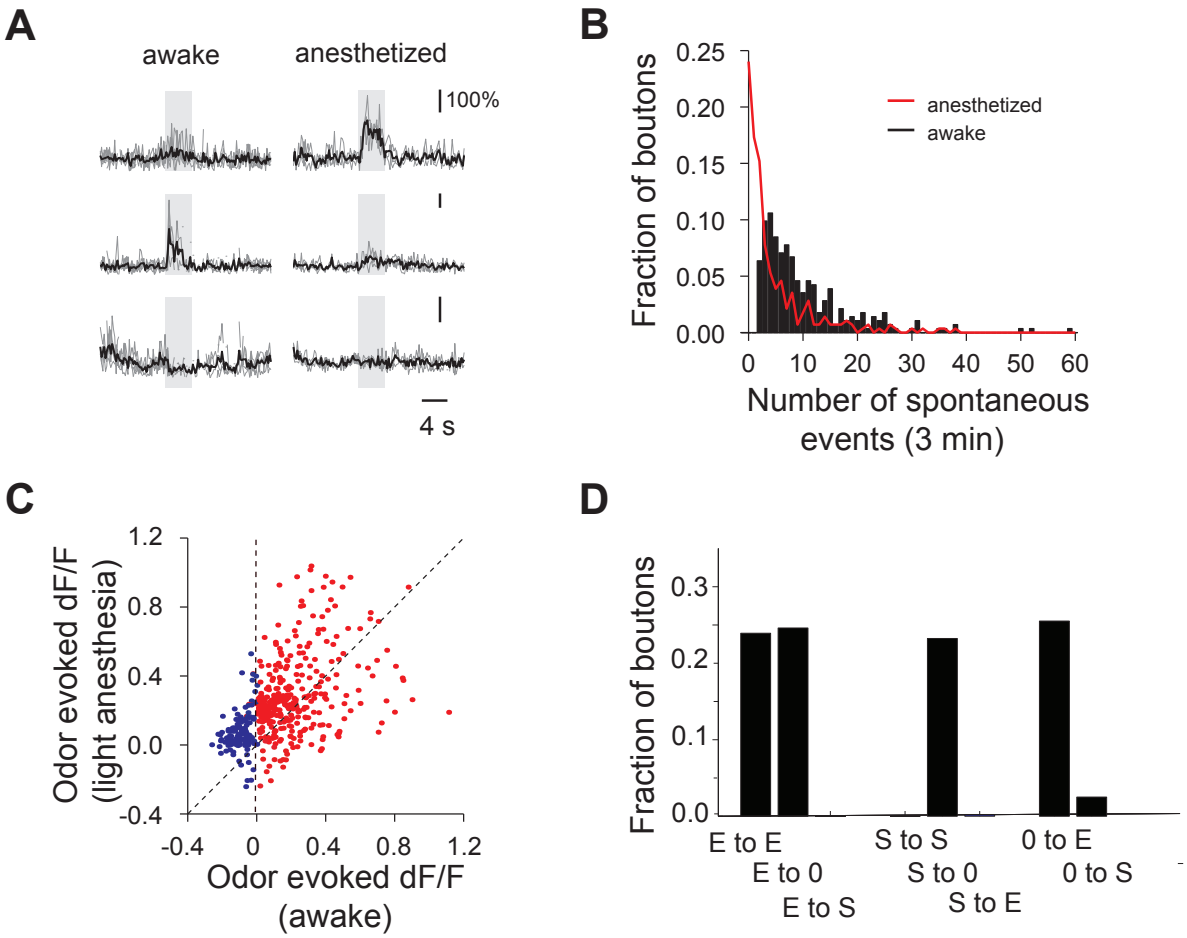
A
awake
anesthetized
100%
4 s
B
Fraction of boutons
0.25
0.20
0.15
0.10
0.05
0.00
anesthetized
awake
0
10
20
30
40
50
60
Number of spontaneous events (3 min)
C
Odor evoked dF/F (light anesthesia)
1.2
0.8
0.4
0.0
-0.4
-0.4
0
0.4
0.8
1.2
Odor evoked dF/F (awake)
D
Fraction of boutons
0.3
0.2
0.1
0.0
E to E
E to 0
E to S
S to S
S to 0
S to E
0 to E
0 to S

Figure S4

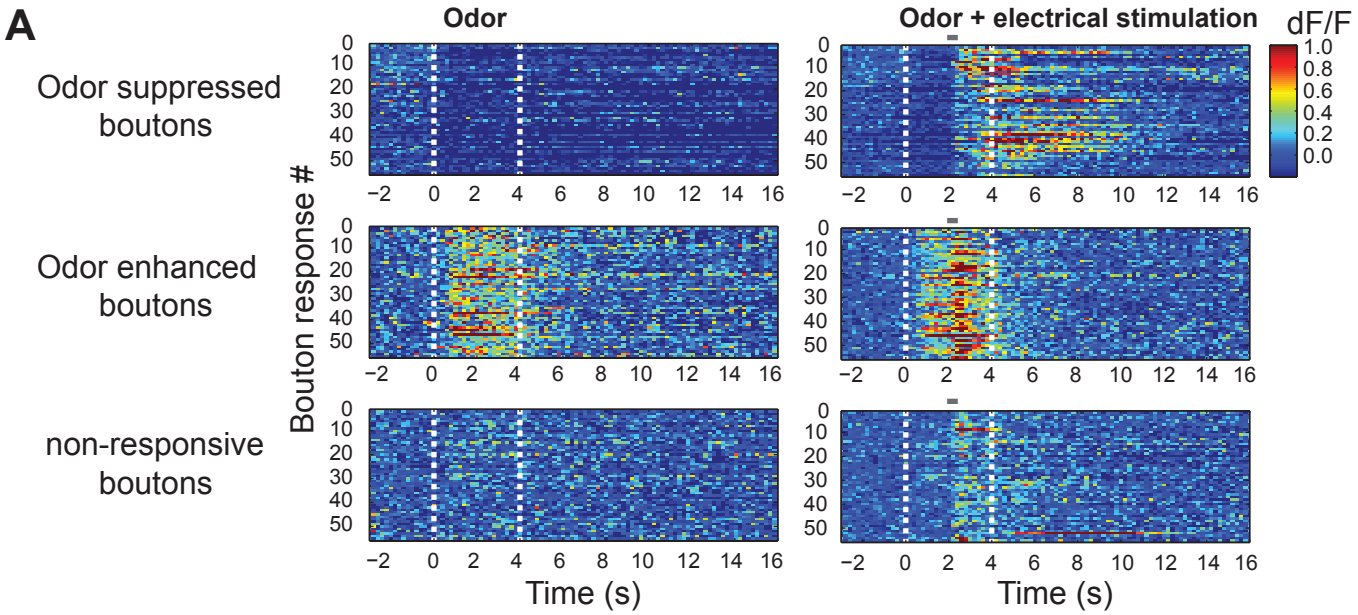
A
Odor
Odor + electrical stimulation
dF/F
Odor suppressed boutons
Odor enhanced boutons
non-responsive boutons
Bouton response #
Time (s)
Time (s)

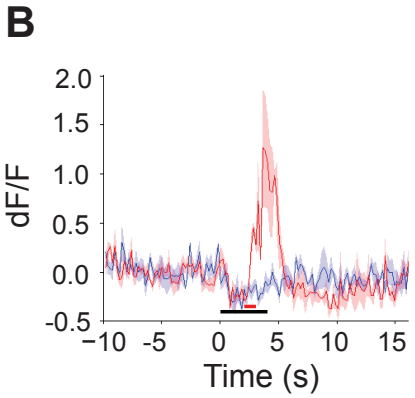
B
dF/F
Time (s)

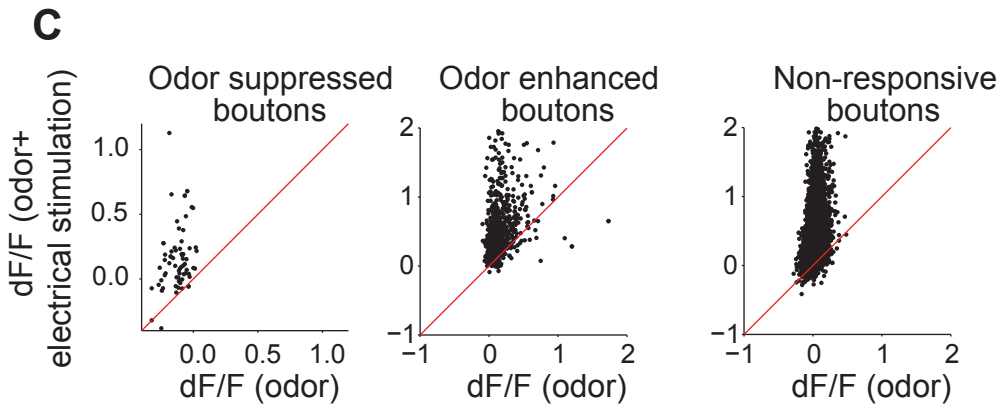
C
Odor suppressed boutons
Odor enhanced boutons
Non-responsive boutons
dF/F (odor+ electrical stimulation)
dF/F (odor)
dF/F (odor)
dF/F (odor)

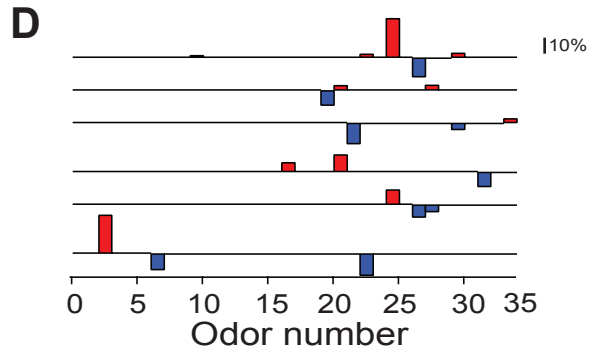
D
10%
Odor number

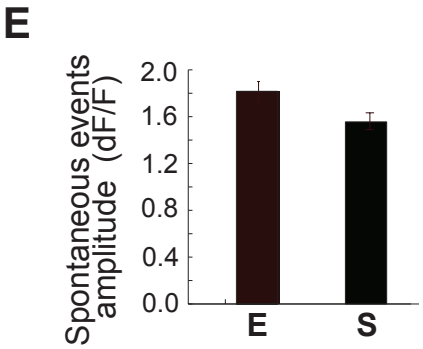
E
Spontaneous events amplitude (dF/F)
E
S

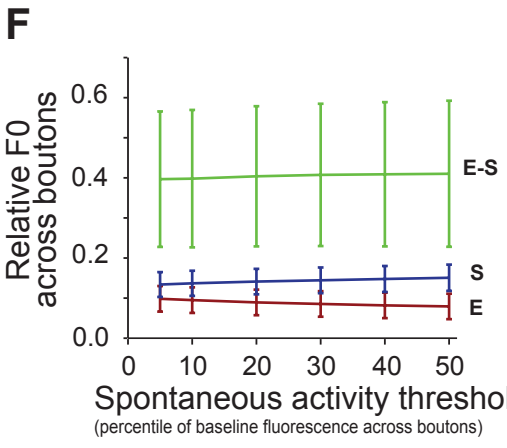
F
Relative F0 across boutons
E-S
S
E
Spontaneous activity threshold
(percentile of baseline fluorescence across boutons)

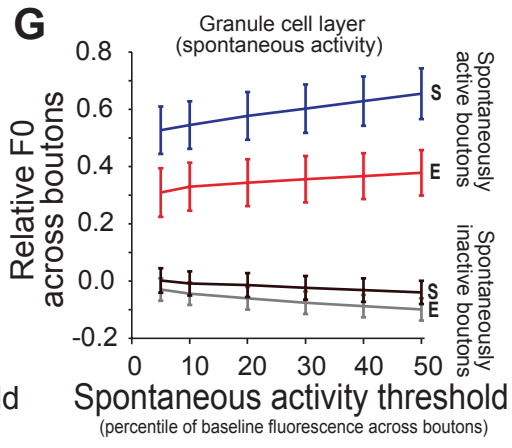
G
Granule cell layer
(spontaneous activity)
Relative F0 across boutons
Spontaneously active boutons
Spontaneously inactive boutons
S
E
S
E
Spontaneous activity threshold
(percentile of baseline fluorescence across boutons)

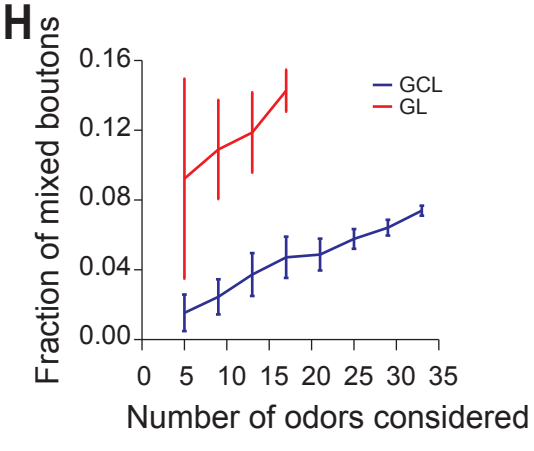
H
Fraction of mixed boutons
GCL
GL
Number of odors considered

Figure S5

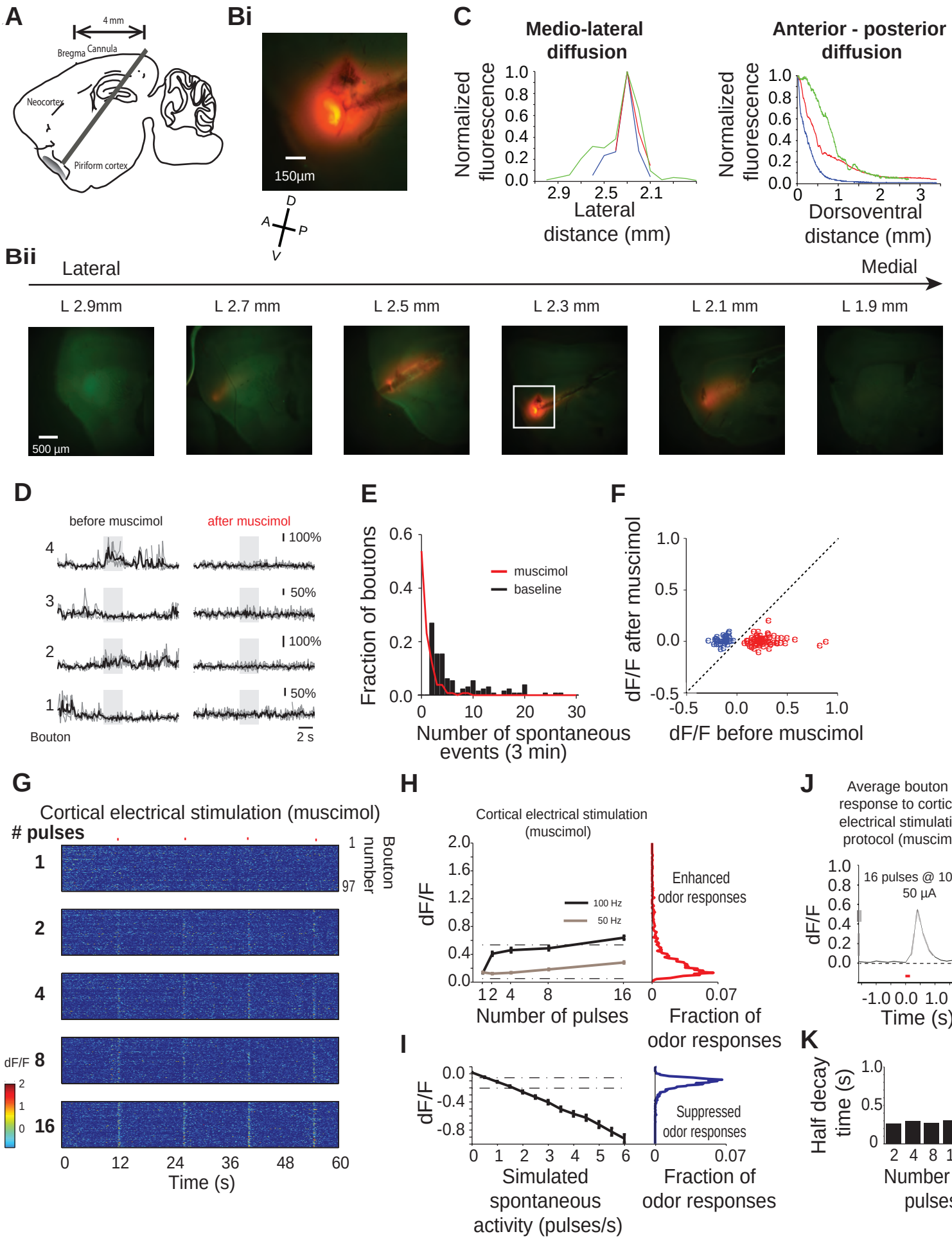
A
4 mm
Bregma
Cannula
Neocortex
Piriform cortex
Bi
150µm
D
A
P
V
C
Medio-lateral diffusion
Normalized fluorescence
1.0
0.8
0.6
0.4
0.2
0.0
2.9
2.5
2.1
Lateral distance (mm)
Anterior - posterior diffusion
Normalized fluorescence
0
1
2
3
Dorsoventral distance (mm)
Bii
Lateral
Medial
L 2.9mm
L 2.7 mm
L 2.5 mm
L 2.3 mm
L 2.1 mm
L 1.9 mm
500 µm
D
before muscimol
after muscimol
4
3
2
1
100%
50%
100%
50%
Bouton
2 s
E
Fraction of boutons
0.6
0.4
0.2
0.0
muscimol
baseline
0
10
20
30
Number of spontaneous events (3 min)
F
dF/F after muscimol
1.0
0.5
0.0
-0.5
-0.5
0.0
0.5
1.0
dF/F before muscimol
G
Cortical electrical stimulation (muscimol)
pulses
1
2
4
8
16
1
97
Bouton number
dF/F
2
1
0
0
12
24
36
48
60
Time (s)
H
Cortical electrical stimulation (muscimol)
dF/F
2.0
1.6
1.2
0.8
0.4
0.0
100 Hz
50 Hz
Enhanced odor responses
12 4
8
16
0
0.07
Number of pulses
Fraction of odor responses
J
Average bouton response to cortical electrical stimulation protocol (muscimol)
16 pulses @ 100 Hz
50 µA
dF/F
1.0
0.8
0.6
0.4
0.2
0.0
-1.0 0.0 1.0 2.0
Time (s)
I
dF/F
0.0
-0.4
-0.8
Suppressed odor responses
0 1 2 3 4 5 6
0
0.07
Simulated spontaneous activity (pulses/s)
Fraction of odor responses
K
Half decay time (s)
1.0
0.5
0
2 4 8 16
Number of pulses

Figure S6

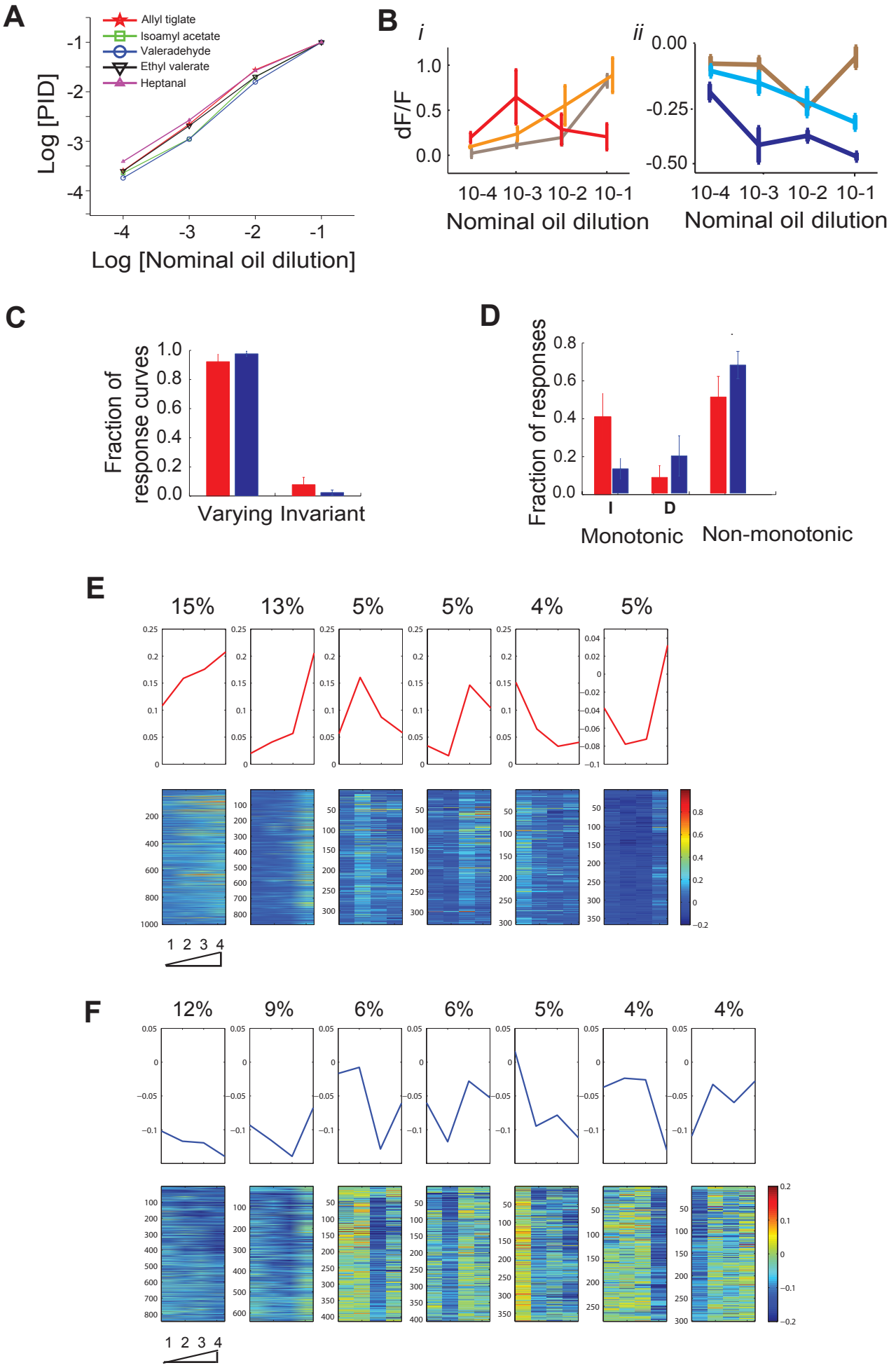
A
Allyl tiglate
Isoamyl acetate
Valeradehyde
Ethyl valerate
Heptanal
Log [PID]
Log [Nominal oil dilution]
B
i
ii
dF/F
Nominal oil dilution
Nominal oil dilution
C
Fraction of response curves
Varying
Invariant
D
Fraction of responses
I
D
Monotonic
Non-monotonic
E
15%
13%
5%
5%
4%
5%
1 2 3 4
F
12%
9%
6%
6%
5%
4%
4%
1 2 3 4

Figure S7

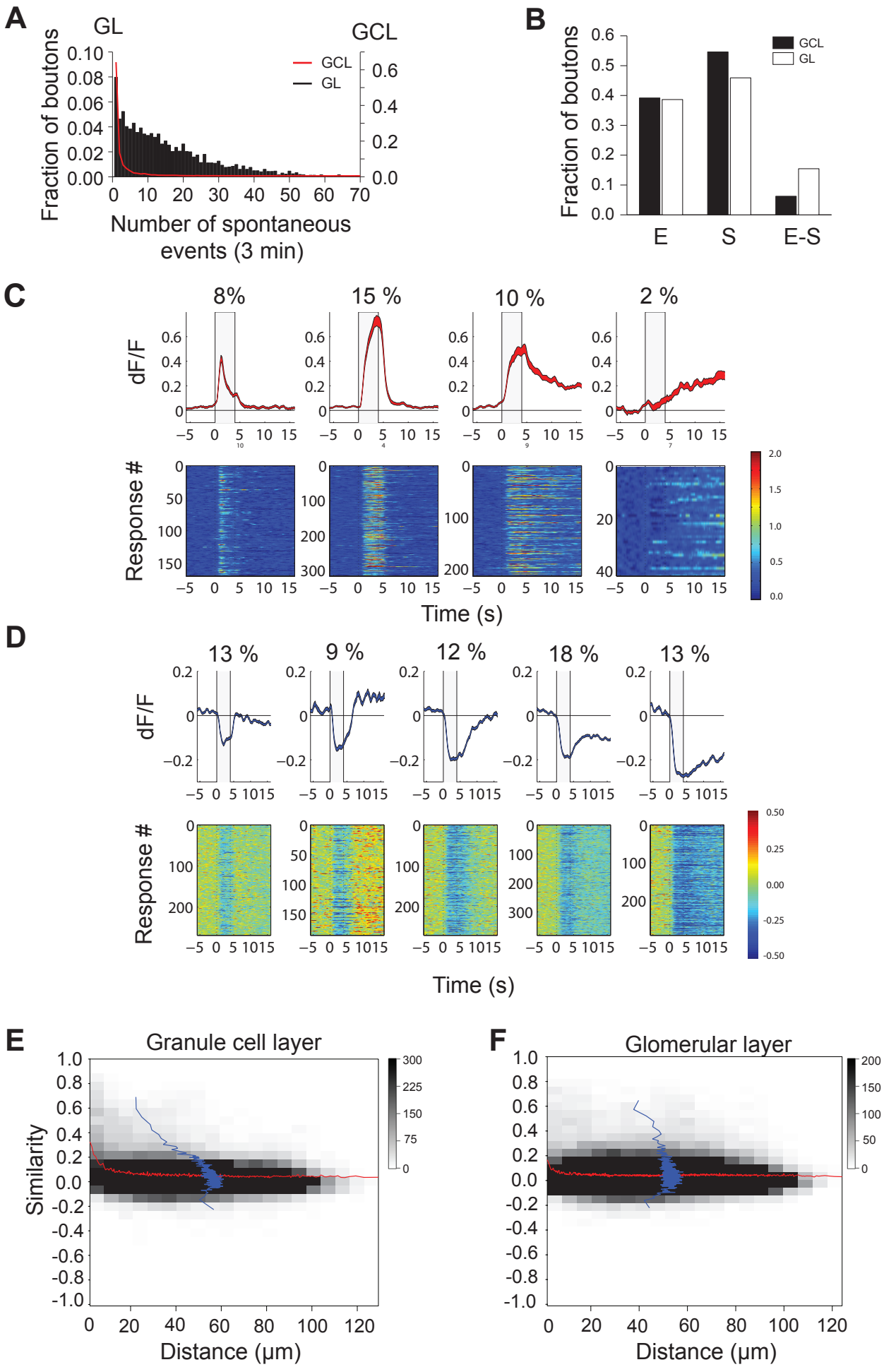
A
GL
GCL
Fraction of boutons
GCL
GL
Number of spontaneous events (3 min)
B
Fraction of boutons
GCL
GL
E
S
E-S
C
8%
15 %
10 %
2 %
dF/F
Response #
Time (s)
D
13 %
9 %
12 %
18 %
13 %
dF/F
Response #
Time (s)
E
Granule cell layer
Similarity
Distance (μm)
F
Glomerular layer
Distance (μm)

Figure S8

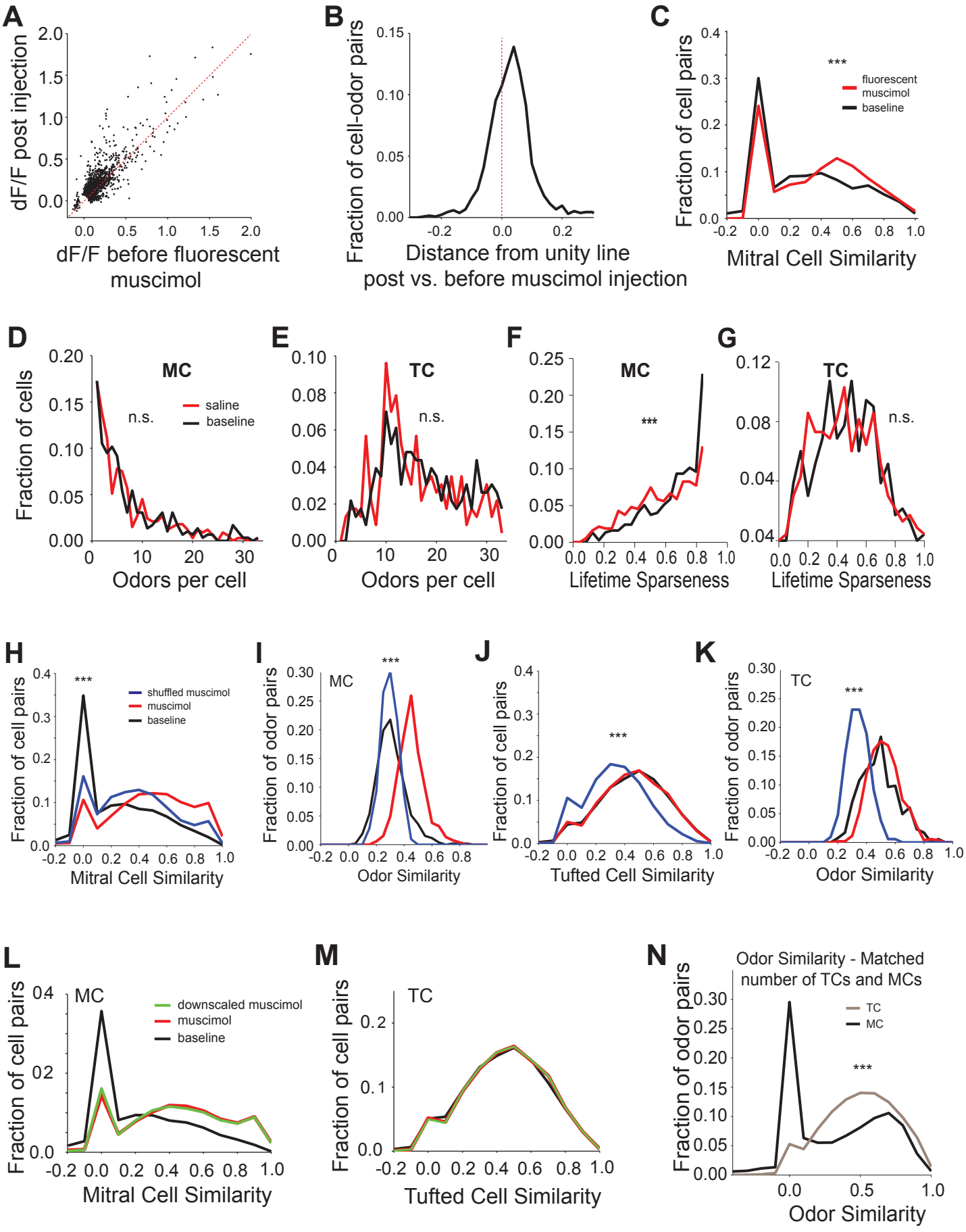
A
dF/F post injection
dF/F before fluorescent muscimol
B
Fraction of cell-odor pairs
Distance from unity line
post vs. before muscimol injection
C
Fraction of cell pairs
***
fluorescent muscimol
baseline
Mitral Cell Similarity
D
MC
n.s.
saline
baseline
Fraction of cells
Odors per cell
E
TC
n.s.
Odors per cell
F
MC
***
Lifetime Sparseness
G
TC
n.s.
Lifetime Sparseness
H
***
shuffled muscimol
muscimol
baseline
Fraction of cell pairs
Mitral Cell Similarity
I
MC
***
Fraction of odor pairs
Odor Similarity
J
***
Fraction of cell pairs
Tufted Cell Similarity
K
TC
***
Fraction of odor pairs
Odor Similarity
L
MC
downscaled muscimol
muscimol
baseline
Fraction of cell pairs
Mitral Cell Similarity
M
TC
Fraction of cell pairs
Tufted Cell Similarity
N
Odor Similarity - Matched number of TCs and MCs
TC
MC
***
Fraction of odor pairs
Odor Similarity

Supplemental Items Legends

Figure S1 relates to Figure 1 and Experimental Procedures.

Figure S2 relates to Experimental Procedures.

Figure S3 relates to Figure 1.

Figure S4 relates to Figure 1.

Figure S5 relates to Experimental Procedures and Figures 5-7.

Figure S6 relates to Figure 2.

Figure S7 relates to Figures 3 and 4.

Figure S8 relates to Figures 5-7.

Movie S1: "Corticalbulbar feedback boutons spontaneous activity" refers to Figure 1.

Movie S2: "Example corticalbulbar feedback boutons enhanced and suppressed responses to ethyl tiglate" refers to Figure 2.

Movie S3: "Example corticalbulbar feedback boutons enhanced and suppressed responses to acetal" refers to Figure 2.

Movie S4: "Example mitral cells responses to 4-heptanone before and after suppression of piriform cortex via muscimol" refers to Figure 5.

Movie S5: "Example tufted cells responses to methyl tiglate before and after suppression of piriform cortex via muscimol" refers to Figure 6.

Table 1 refers to Experimental Procedures.

Supplemental Note 1 refers to Experimental Procedures.

Supplemental Figure Legends

Figure S1. Viral labeling of corticobulbar feedback axons and algorithms for motion detection during imaging in awake head-fixed mice.

A. GCaMP5 expression in APC cell bodies: DAPI nuclear (blue) signals, cytosolic GCaMP5 (green) and composite of the two from confocal single optical slice (*Top*) and maximum projection (*Bottom*) reconstructions; fixed sagittal brain slice from a mouse injected into the anterior piriform cortex (APC) with AAV GCaMP5 expressing viruses;

B. Lack of GABAergic APC projections to the OB: composite DAPI nuclear (blue) signals and cytosolic GCaMP5 (green) images from fixed sagittal slices in APC and OB (GL, MCL and GCL) in a *GAD65*-Cre mouse injected with an *EF1-DIO-GCaMP5* AAV virus in the APC;

C. (*Left*) Example OB sagittal slice from a mouse infected with GCaMP5 in the anterior piriform cortex; (*Right*) zoom-in to glomerular layer (GL), external plexiform layer (EPL) and granule cell layer (GCL);

D. Density of fluorescently labeled (GCaMP5) boutons in the GL, EPL and GCL (boutons/μm^2); solid bars – fixed tissue; open bars – *in vivo*;

E. Example field of view in the granule cell layer and example single bouton (inset) for motion detection analysis; average reference (*Top*), as well as stable (*Bottom Left*) and x-y-z shifted frame (*Bottom Right*) are shown;

F. Uncentred correlation coefficient for each ROI between the average reference and individual frames across the duration of the trial; 0 marks the start of odor presentation; color scalebar shows correlation values;

G. Population stability for the field of view shown in E, during the same example trial, defined as the median of the distribution of correlation coefficients across all ROIs in the field of view; dotted line marks the threshold for determining x-y-z movement; note deflections below threshold classified as motion artifacts by the algorithm;

H. (*Left*) Example field of view ~300 µm deep from OB surface of GCaMP5 labeled cortical feedback axons and boutons in an awake head-fixed mouse; (*Right*) Spontaneous activity traces (dF/F_0) from the feedback boutons marked in the example FOV. Top five traces and respectively bottom three traces are from boutons assigned to two axonal branches by reconstruction of single axons;

Figure S2. Strategies for detection of spontaneous events and significant odor responses in corticobulbar feedback boutons.

A. Example normalized spontaneous fluorescence fluctuations (arbitrary units) from an example feedback bouton during a three minutes period preceding odor presentation; dotted red line indicates the threshold for detection of spontaneous events;

B. Histogram of fluorescence values (arbitrary units) in the time interval shown in **A**. (black bars) and log-normal distribution fit (red trace).Vertical red bar marks the 99th percentile of the fitted distribution and represents the detection threshold for spontaneous events; F_0 is the median of the fluorescence signal in the recorded interval;

C, D. Example spontaneous fluorescence fluctuations across 60 repeats of one enhanced (**C**) and one suppressed (**D**) feedback bouton during a 10 seconds period preceding odor presentation, as well as during three repeats of same stimulus presentation (4 s) and recovery period (12s).

E, **F**. Histogram of values (arbitrary units) in the pre-odor intervals shown in **C.** and **D**. Red bars correspond to the 99.9^{th} /0.1^{th} percentile of the recorded spontaneous fluorescence fluctuations distribution and represent the signal threshold. Blue bars mark the average single trial fluorescence during odor presentation;

G. Histogram of the number of odors that individual feedback boutons imaged in the GCL responded to (black bars) and binomial fit (red line).

H. Logarithmic plot showing the relationship between average number of odors per bouton data (black bars) shown in **G.** and the binomial fit (red line); note underestimation of the fraction of boutons responding to more than two odors by the binomial fit;

Figure S3. Awake versus anesthetized corticalbulbar feedback bouton responses

A. Responses of three example feedback boutons in an awake vs. lightly anesthetized mouse; Individual trials (gray) and average trace (black) are shown; shaded box marks odor presentation (4s);

B. Histogram of average number of spontaneous events (dF/F_0) detected in three minute intervals preceding odor stimulation in the awake (black) and anesthetized (red) conditions;

C. Scatter plot showing odor induced changes in bouton fluorescence (dF/F) in awake vs. anesthetized conditions; each dot indicates the response of a given bouton to a given odor (bouton-odor pair) in the awake versus anesthetized condition; only bouton-odor pairs that were detected as significant in at least one of the two conditions are shown; dotted line marks slope of

1; colors indicate bouton responses that were classified as suppressed (blue) and enhanced (red) in the awake condition;

D. Summary of changes in enhanced (E, *Left*) suppressed (S, *Center*) and unresponsive (0, *Right*) feedback bouton fraction of odor responses between awake and anesthetized conditions; E to S, enhanced to suppressed transitions, S to E, suppressed to enhanced response transitions, 0 to E, unresponsive to enhanced response transitions;

Figure S4A-C. Characterization of responses of odor enhanced, suppressed and non-responsive feedback boutons to APC electrical stimulation. Comparison of spontaneous fluorescence of enhanced vs. suppressed feedback boutons.

A. Average responses (3 repeats) of 58 example boutons to 'odors' (*Left*) and 'odor + brief cortical electrical stimulation' (8 pulses, 100μs at 100Hz) (*Right*) delivered interleaved; (*Top*) Odor suppressed boutons; (*Middle*) Odor enhanced boutons; (*Bottom*) Non-responsive boutons to odors in the panel; dotted white lines mark odor stimulation; red line marks electrical stimulation;

B. Example bouton response to an 'odor' (blue) and 'odor + cortical electrical stimulation' (red); note switch of response polarity from 'suppressed' to 'enhanced'; black line marks odor stimulation; red line marks electrical stimulation;

C. Scatter plots showing odor induced change in bouton fluorescence (dF/F) in the absence and presence of cortical electrical stimulation; each dot indicates the response of a given bouton to a given odor (bouton-odor pair) in the absence versus presence of cortical electrical stimulation; red line marks slope of 1;

D. Example odor response spectra of six feedback boutons showing both enhancement, as well as suppression of baseline activity in response to presentation of odors (Odor Set B, Table S1);

E. Average amplitude of spontaneous events excursions from baseline fluorescence (F_0) for odor enhanced (E) and respectively suppressed (S) boutons;

F. Relative baseline fluorescence (F_0), (see Methods) as a function of varying the detection threshold for spontaneous events; relative baseline fluorescence for enhanced (red), suppressed (blue) and mixed (green) boutons are shown; 640 suppressed, 564 enhanced, 41 mixed boutons; error bars represent SEM across boutons;

G. Relative baseline fluorescence (F_0) as a function of varying the detection threshold for boutons classified as spontaneously active (top two traces) and spontaneously inactive (bottom two traces); Relative baseline fluorescence (F_0) corresponding to spontaneously active and odor enhanced (red, 165 boutons), spontaneously active and odor suppressed (blue, 214 boutons), spontaneously inactive and odor enhanced (gray, 399 boutons) and spontaneously inactive, odor suppressed (black, 426 boutons) boutons are shown; error bars represent standard deviation of the mean across boutons, SD;

H. Average percentage of odors in the panel (Odor Set A and B, Table S1) a given mixed bouton responds to as a function of the number of odors presented; quantification for boutons in the GL (red) and GCL (blue) are shown; error bars represent standard deviation of the mean across boutons, SD.

Figure S5. Visualizing the spread of fluorescent muscimol injection, characterization of piriform cortex pharmacological suppression on feedback boutons activity, and

relationship between electrical stimulation and bouton fluorescence changes after piriform cortex inactivation.

A. Cartoon of sagittal brain slice illustrating the position of cannula used for muscimol infusion into APC; distance from the bregma is marked;

Bi. Spread of muscimol at the fluorescent muscimol injection site. **Bii.** Six representative slice examples, located 0.6 mm lateral to and 0.4 mm lateral from the fluorescent muscimol injection site (0), illustrating the position of the injection site within the APC and spread of red fluorescent muscimol; A-anterior, P-posterior, D-dorsal, V-ventral;

C. Distribution of fluorescence intensity decay with increasing distance from the injection site for the medial-lateral axis (*Left*) and anterior-posterior axis (*Right*) normalized to average fluorescence at the injection site;

D. Responses of four example boutons before and after muscimol injection in the APC; Individual trials (gray) and average trace (black) are shown; shaded box marks odor presentation (4s);

E. Histogram of average number of spontaneous events detected in three minute intervals preceding odor stimulation before (black) and after (red) muscimol injection;

F. Scatter plot showing odor induced change in bouton fluorescence (dF/F) before and after muscimol injection; each dot indicates the response of a given bouton to a given odor (bouton-odor pair) before versus after drug injection; only bouton-odor pairs that were detected as significant in at least one of the two conditions are shown; dotted line marks slope of 1; colors indicate bouton responses that were classified as suppressed (blue) and enhanced (red) before muscimol injection;

G. Responses (dF/F) of 100 example cortical feedback boutons to 4 repeats of different cortical electrical stimulation protocols (1-16 pulses, 100μs at 100Hz);

H. (*Left*) Average bouton response amplitude to five protocols of cortical electrical stimulation in the presence of muscimol at 50Hz (grey) and 100Hz (black); (*Right*) Distribution of bouton fluorescence changes (enhanced responses, dF/F) to odors in the panel (Odor Set A, Table S1);

I. (*Left*) Estimate of suppression in baseline average fluorescence, given a range of different simulated spontaneous activity (by convolving the average bouton response to electrical stimulation with a Poisson pulse train, see Methods); (*Right*) Distribution of bouton fluorescence changes (suppressed responses, dF/F) to odors in the panel (Odor Set A, Table S1);

J. Average bouton fluorescence change in response to cortical electrical stimulation (16 pulses, 100μs, 100 Hz) in the presence of muscimol;

K. Offset kinetics (half decay time) of average bouton responses to four protocols of cortical electrical stimulation in the presence of muscimol.

Figure S6. Characterization of corticobulbar feedback responses across odor concentrations.

A. Log-log plot showing the relationship between nominal dilutions in mineral oil to relative odor concentrations in air measured using a photo-ionization detector (PID) device; different color traces represent different odors: allyl tiglate, isoamyl acetate, valeraldehyde, ethyl valerate and heptanal;

B. Enhanced (*i*) and suppressed (*ii*) concentration–response (GCaMP5) curves for three example boutons each to two different odors (*i*, *ii*) in cortical feedback boutons; error bars indicate SEM across repeats;

C. Fraction of varying and invariant bouton odor responses within the sampled concentration range; enhanced (red) and suppressed (blue) bouton responses are shown;

D. Fraction of monotonical and non-monotonical changes in odor response amplitude within the concentration range for individual boutons; enhanced (red) and suppressed (blue) bouton responses are shown; *I*, monotonically increasing responses with increasing concentration; *D*, monotonically decreasing responses with increasing concentration;

E, F. Odor concentration response curves types obtained using k-means clustering and their relative distribution in the population of cortical feedback boutons targeting GCL; Average response shapes (*Top*) and all corresponding odor responses (GCaMP5) assigned to each cluster (*Bottom*) **E.** Enhanced response clusters; **F.** Suppressed response clusters; Color scale bars indicate average dF/F;

Figure S7. Characterization of corticobulbar feedback responses in the glomerular layer of the olfactory bulb.

A. Histogram of average number of spontaneous events detected above fluorescence baseline (F_0) in a three minute interval preceding odor stimulation; distributions in the GCL (black bars) and GL (red trace) are shown;

B. Fraction of boutons that responded significantly to odors in the panel (Odor Set A, Table S1) via only enhancement (E), only suppression (S) and both enhancement and suppression (E-S) across all responsive boutons sampled in the granule cell layer, GCL (solid bars) and glomerular layer, GL (open bars).

C, D. Odor response types obtained via k-means clustering and their relative distribution in the population of feedback boutons targeting the GL; Average response shapes (*Top*) and all

corresponding odor responses (GCaMP5) assigned to each cluster (*Bottom*) **A.** Enhanced response clusters; **B.** Suppressed response clusters; Color scale bars indicate average dF/F;

E, F. Two-dimensional histogram of pairwise correlations between spontaneous activity fluctuations of individual boutons in the granule cell layer (**E**) and glomerular layer (**F**) versus their physical separation. Red, average similarity (pairwise correlation) across different inter-bouton distances; Blue, average inter-bouton distance across all similarity values of bouton pairs; Gray scale, number of pairs per bin.

Figure S8. Odor responsiveness and population correlations of mitral and tufted cells before and after muscimol (non-fluorescent and fluorescent) injection in the anterior piriform cortex (APC).

A. Scatter plots showing odor induced change in mitral cell body fluorescence (dF/F) before and after *fluorescent muscimol*; each dot indicates the response of a given cell to a given odor (cell-odor pair) before versus after drug injection; only cell-odor pairs that were detected as significant in at least one of the two conditions are shown; dotted line marks slope of 1;

B. Summary histogram showing change in odor evoked mitral cells responses upon *fluorescent muscimol* (black) injection compared to pre-injection baseline; the change for each mitral cell odor response (each dot in **G**) is quantified in terms of the Euclidian distance from the diagonal unity line (dotted line indicating slope of 1);

C. Histogram of pairwise cell similarity of mitral cells before (black, baseline) and after (red) *fluorescent muscimol* injection ('baseline' MC Similarity=0.29 ± 0.004 vs. 'post-fluorescent muscimol' MC Similarity = 0.38 ± 0.004, N = 6,048 MT- odor pairs); Odor Set B, Table S1; *** indicate significance level ($p<0.001$, Wilcoxon signed rank test);

D. Histogram of the number of odors that individual mitral cells responded to before (black trace) and after (red trace) saline injection; (Avg. number of odor responses per cell = 7.32 ± 0.02 pre-saline vs. 6.99 ± 0.02 post-saline, N = 333 MCs, 4 hemibulbs, Wilcoxon sign rank test, p=0.12);

E. Histogram of the number of odors individual tufted cells responded to before (black trace) and after (red trace) saline injection; (Avg. number of odor responses per cell = 17.40 ± 0.30 pre-saline vs. 15.63 ± 0.15 post-saline, N = 229 TCs, 4 hemibulbs, Wilcoxon sign rank test, p=1);

F. Histogram of lifetime sparseness values for individual mitral cells before (black trace) and after (red trace) saline (Avg. lifetime sparseness = 0.78 ± 0.01 pre-saline vs. 0.69 ± 0.01 post-saline, N = 375 MCs, 4 hemibulbs, Wilcoxon sign rank test, p< 0.001, **I**) injection; *** indicate significance level (p<0.001, Wilcoxon signed rank test);

G. Histogram of lifetime sparseness values for individual tufted cells before (black trace) and after (red trace) saline (Avg. lifetime sparseness = 0.47 ± 0.01 pre-saline vs. 0.45 ± 0.01 post-saline, N = 233 TCs, 4 hemibulbs, Wilcoxon sign rank test, p< 0.001, **K**) injection; *** indicate significance level (p<0.001, Wilcoxon signed rank test); n.s. – not significant;

H. Histogram of pairwise cell similarity of mitral cells before (black, baseline), after (red) muscimol injection, as well as shuffled odor index control (blue) after muscimol injection; *** indicate significance level (Avg. MC Similarity=0.49 ± 0.002 vs. Avg. Shuffled MC Similarity = 0.36 ± 0.001, N=27,391 MT- odor pairs. Wilcoxon signed rank test, p<0.001);

I. Histogram of pairwise odor similarity of mitral cells before (black) and after (red) muscimol injection, as well as shuffled cell index control (blue) after muscimol injection; *** indicate significance level (Avg. MC Odor Similarity = 0.45 ± 0.01 vs. Shuffled Avg. MC Odor Similarity = 0.29 ± 0.002, p<0.001, Wilcoxon signed rank test, p<0.001);

J. Histogram of pairwise cell similarity of tufted cells before (black, baseline) and after (red) muscimol injection, as well as shuffled odor index control (blue) after muscimol injection (Avg. TC Similarity = 0.47 ± 0.002 vs. Avg. Shuffled TC Similarity = 0.34 ± 0.004, 11,522 TC-odor pairs. Wilcoxon signed rank test, $p<0.001$);

K. Histogram of pairwise odor similarity of tufted cells before (black), after (red) muscimol injection and shuffled cell index control (blue) after muscimol injection; (Avg. TC Odor Similarity = 0.53 ± 0.003 vs. Shuffled Avg. MC Odor Similarity = 0.34 ± 0.003, $p<0.001$, Wilcoxon signed rank test); *** indicate significance level.

L. Histogram of pairwise cell similarity of mitral cells before (black, baseline), after (red) muscimol injection, as well as 'downscaled-muscimol' control (green, see Methods) after muscimol injection; Avg. MC Similarity Muscimol=0.44 ± 0.002 vs. Avg. MC Similarity Downscaled Muscimol = 0.43 ± 0.002, N=22,654 MC- odor pairs; Wilcoxon rank sum test, $p>0.05$);

M. Histogram of pairwise cell similarity of tufted cells before (black, baseline) and after (red) muscimol injection, as well as 'downscaled-muscimol' control (green) after muscimol injection (Avg. TC Similarity Muscimol = 0.46 ± 0.002 vs. Avg. TC Similarity Downscaled Muscimol = 0.46 ± 0.002, 9,532 TC-odor pairs. Wilcoxon ranksum rank test, $p > 0.05$);

N. Histogram of pairwise odor similarity of mitral cells (black, MC) and tufted cells (gray, TC) before muscimol injection matched in numbers in terms of cells considered per field of view (40 randomly picked cells per field of view, 9 fields of view per iteration, 20 iterations); *** indicate significance level (Avg. MC Odor Similarity = 0.31 ± 0.001,N=94,402 odor pairs vs. Avg. TC Odor Similarity = 0.50 ± 0.001, N=73,561 odor pairs, $p<0.001$, Wilcoxon rank sum test);

Supplemental Movies

Movie S1

Time series movie acquired for 3 minutes at 5Hz showing the spontaneous activity of cortical feedback boutons expressing GCaMP5 in an optical plane ~300 μm below surface; Speed is 12x real time. Imaging window is 120 μm X 120 μm.

Movie S2

Time series movie showing a single trial response of corticobulbar feedback boutons in the GCL to ethyl tiglate. Within the field of view, odor presentation evoked enhanced (red arrow) and suppressed responses (green arrow). White arrow marks a bouton that did not respond to the odor stimulus. Speed is 2x real time. Imaging window is 110 μm X 75 μm.

Movie S3

Time series movie showing a single trial response of corticobulbar feedback boutons in the GCL to acetal. Within the field of view, odor presentation evoked enhanced (red arrow) and suppressed responses (green arrow). White arrow marks a bouton that did not respond to the odor stimulus. Speed is 2x real time. Imaging window is 110 μm X 75 μm.

Movie S4

Time series movie showing a single trial response (10Hz) of GCaMP3 expressing mitral cells (~220 μm from surface) to 4-heptanone. Odor-evoked responses of mitral cells before (Top) and after (Bottom) muscimol injection in the anterior piriform cortex (APC). Speed is 1x real time. Imaging window is 480 μm X 300 μm.

Movie S5

Time series movie showing a single trial response (10Hz) of GCaMP3 expressing tufted cells (~140 μm from surface) to methyl tiglate. Odor-evoked responses of mitral cells before (Left) and after (Right) muscimol injection in the anterior piriform cortex (APC). Speed is 1x real time. Imaging window is 300 μm X 480 μm.

Table S1

Odor index	Odor Set A	Odor Set B	Concentration
1	Acetal	2,4 decadienal	Allyl tiglate
2	1,4 Cineole	Propyl tiglate	Isoamyl acetate
3	Gamma Terpinene	valeraldehyde	Valeraldehyde
4	p-anis aldehyde	2,3-Pentanedione	Ethyl Valerate
5	Hexanal	Ethyl hexanoate	Heptanal
6	Methyl piruvate	Allyl butyrate	
7	Heptanal	Ethyl valerate	
8	Ethyl tiglate	2,3-Diethylpyrazine	
9	Valeraldehyde	hexanal	
10	2,3 pentanedione	Ethyl heptanoate	
11	Allyl tiglate	heptanal	
12	Ethyl propionate	Allyl tiglate	
13	1,4 dimethoxybenzene	ethyl tiglate	
14	Verbenone	Isoamyl acetate	
15	Ethyl butyrate	Methyl tiglate	
16	Citral	ethyl 3-mercapto propionate	
17	Ethyl valerate	4-heptanone	
18	(S)-limonene	gamma terpinene	
19	Ethyl caproate	Ethyl propionate	
20	Isoamyl acetate	acetal	
21		Ethyl butyrate	
22		1-pentanol	
23		acetophenone	
24		cyclohexyl acetate	
25		4-isopropyl benzaldehyde	
26		propyl acetate	
27		1-propanethiol	
28		cineole	
29		2-hexanone	
30		isobutyl propionate	
31		Hexanoic acid	
32		1,3 dimethoxybenzene	
33		valeric acid	

Supplemental Note 1

Cortical feedback boutons responded to odors either via either enhancement or suppression of baseline fluorescence, the mixed boutons (showing both enhanced, as well as suppressed responses) being a small minority. Could this dichotomy be explained simply by baseline saturation (due to high spontaneous activity) in the case of suppressed boutons which may prevent the detection of enhanced odor responses? Or, alternatively, by low fluorescence baseline in the case of enhanced boutons which would make the detection of small odor suppressed responses challenging? Several lines of evidence suggest that these issues are unlikely explanations for the observed response dichotomy across cortical feedback boutons.

a) in both enhanced and suppressed boutons, we observed robust spontaneous excursions in three minutes intervals recorded before odor stimulation (for both types, Avg. Amplitude of spontaneous events > 150 % dF/F_0) with respect to resting fluorescence (F_0) (Figure S4E); therefore, the baseline fluorescence signal is not already saturated at rest in the case of the suppressed boutons and affords in principle the detection of positive deflections;

b) Baseline fluorescence (F_0) was on average higher for suppressed vs. enhanced boutons, consistent with our observation of higher levels spontaneous activity in the suppressed boutons and the conservative threshold chosen for the detection of 'spontaneous events'; if a high pedestal of baseline fluorescence is an important limitation in the detection of 'enhanced' responses, then it is expected that on average the baseline fluorescence of mixed boutons (showing both types of responses) lies between that of purely suppressed and purely enhanced boutons. This was not the case: consistently, mixed boutons displayed on average higher baseline fluorescence (F_0) compared to both suppressed and enhanced boutons, irrespective of the detection threshold chosen for calling 'spontaneous events' (Figure S4F);

c) baseline fluorescence (F_0) was on average lower for boutons classified as spontaneously inactive vs. active, which may reflect the conservative nature of our detection threshold; importantly, baseline fluorescence of 'spontaneously active enhanced boutons' was higher than that of 'spontaneously inactive suppressed boutons', suggesting that the baseline fluorescence of 'spontaneously active enhanced boutons' was in principle high enough to afford the detection of suppressed odor responses had there been any (Figure S4G);

d) cortical feedback boutons in the glomerular layer showed robust spontaneous activity, more so than boutons in the granule cell layer (GCL); however, the feedback boutons in the glomerular layer were significantly sparser in suppressed odor responses compared to those in the GCL. The higher frequency of spontaneous events in the glomerular layer can be in principle related to differences in laser power and ease of optical access to the glomerular layer. Had high baseline fluorescence been a determining factor for detecting suppressed events, it is expected that the feedback boutons in the GL showed an increased frequency of suppressed odor responses, due to superior detectability. In fact, suppressed responses in the GL were sparser compared to those in the GCL (Figure 3D).

Experimental Procedures

Surgical Procedures: Adult mice (males and females >30 days old, 25-40 g) were anesthetized with ketamine/xylazine (KX, initial dose 70/7 mg/kg), further supplemented to keep the pedal withdrawal reflex suppressed. Lidocaine was applied topically at the site of surgical incision. Temperature was maintained at 37^{o} C using a heating pad (FST TR-200, Fine Science Tools, USA). Respiratory rate and lack of pain reflexes were monitored throughout the experiment. After the animal was deeply anesthetized, it was mounted in a stereotaxic frame with ear bars. Lidocaine and iodine were applied topically to skin (as analgesic and antiseptic, respectively). Aseptic technique was used, first clipping hair and prepping with betadine on the skin. Eyes were covered using paralube. A small incision (2-3 cm) was made into the skin above the surgical site.

Viral expression of GCaMP5 in the anterior piriform cortex (APC): To ensure spatially homogeneous expression, we performed three injections in each piriform cortex hemisphere, along the A-P and M-L axes (1.5 mm lateral, 2.8 mm anterior with respect to bregma, 3.0 mm deep from surface; L 2.0 mm, A 2.2 mm, D 3.5 mm; and respectively L2.5 mmm, A1.8 mm, D 4.0 mm). Post hoc, each imaged brain was perfused in PFA and GCaMP5 expression in the APC and OB assayed in sagittal slices via confocal imaging.

Chronic windows and head-fixed awake multiphoton imaging: Animals were anesthetized as described before and administered dexamethasone (4 mg/Kg) to prevent swelling, enrofloxacin against bacterial infection (5 mg/Kg), and carprofen (5 mg/Kg) to reduce inflammation. To expose the dorsal surface of the OB for chronic imaging, a small craniotomy was made over both OB hemibulbs, using a either a biopsy punch(Adam & Mizrahi, 2011) or thinning the skull with

a high-speed dental drill (Foredom, Bethel, CT), and removing it completely. A 3 mm glass cover slip (CS-3R, Warner Instruments) was placed atop and sealed in place using Vetbond (3M), further reinforced with cyanoacrylate (Krazy Glue) and dental acrylic (Lang Dental). A custom-built titanium head-bar was cemented on the skull near the lambda suture. To increase stability, the head-bar was designed to also contact the skull above the nasal passage, rostral to the OB. During the imaging sessions, the animal's head was held firmly in place by mounting the titanium headbar onto a custom-built holder. Carprofen (5 mg/Kg) was administered for two days following surgery. Animals were left to recover for at least 48 hours after surgery before imaging. GCaMP5 fluorescence was monitored by acquiring optical sections at different depths spanning from the glomerular (65-90 μm from surface) to the granule cell layers (200-350 μm from surface).

Multiphoton imaging: A Chameleon Ultra II Ti:Sapphire femtosecond pulsed laser (Coherent) was coupled to a custom built multiphoton microscope. The shortest optical path was used to bring the laser onto a galvanometric mirrors scanning system (6215HB, Cambridge Technologies). The scanning system projected the incident laser beam tuned at 930 nm through a scan lens (50 mm FL) and tube lens (300 mm FL) to backfill the aperture of the objective. An Olympus 20X, 1.0 NA objective was used for mitral and tufted cell imaging and an Olympus 25X, 1.05 NA for cortical feedback boutons imaging. A Hamamatsu modified H7422-40 photomultiplier tube was used as photo-detector and a Pockels cell (350-80 BK, 302RM driver, ConOptics) as beam power modulator. The current output of the PMT was transformed to voltage, amplified (SR570, Stanford Instruments) and digitized using a data acquisition board that also controlled the scanning (PCI 6115, National Instruments). Image acquisition and scanning (5-10 Hz) were controlled using custom-written software in Labview (National

Instruments). Using submicroscopic beads (0.5 μm) and a 1.05 NA, 25X Olympus objective, the point spread function (PSF) was calculated x-y (1.0 μm FWHM) and z (2.0 μm FWHM). Cortical feedback boutons were imaged across fields of view of either 120 x 120 μm (0.46 μm pixel size) or 60 x 60 μm (0.23 μm pixel size).

Recording procedure: Animals were head-fixed and habituated under the microscope to odors and the sound of the scanning galvos (45 min). Laser power was adjusted to minimize bleaching (<40 mW). For each field of view, 3 minutes of data were acquired before starting odor stimulation.

Data analysis

ROI selection and removal of z-plane motion artifacts

ROIs were manually drawn for individual boutons (0.9-3 μm diameter) in ImageJ using anatomical details from a reference median projection obtained from the 3 minute interval described above. For mitral and tufted cells imaging sessions, ROIs were manually selected based on anatomy. Care was taken to avoid selecting ROIs on cell bodies overlapping with neuropil (M/T lateral dendrites).

To detect fast z-plane movements that might occur across single frames, an average image was calculated using all frames for the given trial. Using this average image, each ROI was described as a vector of length equal to the total number of pixels within the ROI (r_{mean}). We further calculated corresponding vectors from the same ROI across each individual frame (r_{frame}). r_{mean} and r_{frame} were compared by calculating the cosine of the angle between the two vectors:

$$cos_{frame} = \frac{r_{mean} \cdot r_{frame}}{\sqrt{(r_{mean} \cdot r_{mean})(r_{frame} \cdot r_{frame})}}$$

This metric corrects for changes in brightness and only takes into account changes in shape. cos_{frame} has a value of 1, if the ROI in a particular frame is identical in shape to that in the average image, even if dimmer in intensity. If the ROI has a different shape, cos_{frame} approaches zero. Note that, because the ROIs were chosen slightly larger than individual boutons, they included both bright pixels that are part of a bouton, as well as dark pixels from surround. This allowed cos_{frame} to be very sensitive to lateral displacements or z-movements which inevitably change the distribution of bright and dark pixels within the drawn ROI. For each ROI, a time series of cos_{frame} was created that estimated the similarity in time of the bouton to the template average vector. Z-movement for a particular frame would produce a synchronized drop in cos_{frame} across a large number of boutons. We therefore estimated the *population stability* for a given frame as the median of the cos_{frame} calculated over all boutons in a field of view. The *population stability* was converted to a z-score by subtracting the mean population displacement from the air period preceding the odor presentation and dividing by the standard deviation of *population stability* during air. The air period was used to calculate the z-score since we observed only minimal z-movement during this interval. A drop of more than 2 z-scores was classified as a motion artifact and the entire corresponding frame discarded from any further analysis.

Detection of spontaneous events

During the air period, spontaneous increases in fluorescence occurred that deviated from the average fluorescence for a given bouton (ROI). To detect spontaneous events for a given ROI, a distribution of resting fluorescence was constructed, considering only the lower half of the

fluorescence values pooled across 3 minute intervals and fitting it with a log-normal distribution. We assumed that fluorescence values smaller than the median did not overlap with the spontaneous events to be detected, and we used the fitted log-normal distribution as proxy for the distribution of resting fluorescence (99th percentile as threshold for spontaneous events). A spontaneous event was defined as fluorescence transiently crossing the threshold and falling back again to resting values. A bouton was classified as spontaneously active, if at least two spontaneous events were observed during the 3 minute interval. Note that these events likely represent several action potentials and not individual spikes (Tian et al., 2009).

Estimation of relative baseline fluorescence – Figure S$F,G

Generally, the baseline fluorescence was estimated as the median of the distribution of fluorescence signals (50 percentile) for a given bouton. We verified that the analysis shown in Figure S4F and Figure S4G was unaffected even when the threshold was set to lower percentiles. Observed baseline fluorescence for a given field of view depends not only on the intrinsic resting activity, but also on other factors like laser power, tissue scattering etc. To allow comparisons of the estimated baseline fluorescence of boutons acquired across different fields of view, we defined the relative fluorescence of a given ROI in a given field of view as the z-score calculated over the population of all fluorescent boutons in the field of view.

Odor response analysis – detection of significant enhanced and suppressed responses

The distribution of fluorescence for a given ROI is in principle asymmetric, limited by saturation for increases, and 0 firing rate for decreases in fluorescence. Parametric tests of

significance that set symmetric thresholds as a number of standard deviations above and below the mean fluctuation would result in underestimating the significance of suppressed events. Given access to long periods of air recorded preceding odor presentations (20 odors * 4 repeats per odor *10 s per repeat = 800 s per imaging session), we calculated statistics that allowed determining with high confidence whether an increase or decrease in dF/F during odor presentation deviated from spontaneous fluctuations during baseline. We estimated a reference baseline fluorescence distribution by sliding a temporal window of same duration as odor presentation (4s) over the acquired air period and averaging the dF/F. This procedure was repeated 5,000 times to obtain a bootstrap estimate of the spontaneous fluorescence distribution. The response from a single odor repeat was considered 'significant enhancement', if it exceeded 99.9th percentile of the distribution, and respectively 'significant suppression', if it corresponded to less than 0.1th percentile. Note that this procedure is non-parametric, therefore solving the asymmetry problem. An odor was called to trigger significant enhancement (or suppression) for an individual ROI if it elicited responses across at least two repeats.

Functional clustering analysis

In addition to fluorescence changes whose significance was assessed over the 4 s odor period, we also assessed significance during the first 2 s, last 2 s, as well as 4 s following the end of odor presentation. These extra traces were included to capture potential rich temporal dynamics such as early adapting, delayed and OFF responses. The selected waveforms were smoothed using a 0.8 s moving average window and normalized by the absolute value of the largest magnitude response. We used the k-means clustering function in MATLAB (Euclidean distance). Cluster quality was assessed by calculating the average distance between waveforms assigned to a cluster (*d*). To determine the total number of clusters, we calculated the average *d*,

while varying the number of clusters from 2 to 30. The average decrease in *d* was further plotted as a function of increasing number of clusters. The total cluster number (10 for GCL and 9 for GL waveforms) was chosen using a cutoff where the average decrease in *d* plateaued.

Concentration analysis – invariant versus variant responses, monotonicity, clustering

For each ROI, the significance for each odor response at each concentration was assessed independently. An ROI was classified as concentration invariant only if it cleared significance at all four concentrations used and the magnitude of responses did not differ across concentrations. The response at each concentration was described as a vector of mean dF/F during odor period across trials. To construct a concentration response curve, the average dF/F across trials for each concentration was used. Variability across concentrations (q) was quantified as the standard deviation of the trial-averaged dF/F values. A family of concentration response curves was constructed by shuffling the concentration labels for the mean dF/F of individual trials and randomly assigning them to any of the four concentrations used. For each shuffle round, a q' value was obtained by calculating the standard deviation of the resulting concentration response curve. Repeating this procedure 100 times produced a null distribution of q' values. Concentration invariant ROIs were required to have a value of q between the 5th and 95th percentile of the q' distribution.

To establish whether an ROI showed monotonically increasing or decreasing responses to a given odor across concentrations, its concentration response curve (described above) was fitted with a line and its slope evaluated for monotonicity. All odor-ROI pairs that showed at least one significant response (across trials) to at least one of the concentrations were considered. To assess if such a slope could have arisen by chance, a null distribution of slopes (100) was created

by shuffling the concentration labels and calculating shuffled concentration response curves. A response was considered monotonically increasing if its slope was larger than the 95th percentile of the shuffled distribution, and monotonically decreasing if it smaller than the 5th percentile. Clusters of response concentration curves (13) were also calculated using k-means clustering.

Odor pair similarity using enhanced responses only vs. suppressed responses in GL and GCL

Cortical feedback boutons responses separated into boutons that responded only by enhancing or only by suppressing baseline fluorescence. We constructed two vector populations per odor: one using ROIs with purely enhanced responses and one using the purely suppressed ROIs to calculate the Pearson linear correlation coefficient. We also calculated the mutual information (I(e;s)) between the odor similarities obtained using the enhanced population responses versus suppressed responses. The mutual information is given by:

I(e;s)=H(e)+H(s)-H(e,s).

where:

H(e) - entropy of odor similarity distribution using the enhanced responses;

H(i) - entropy of odor similarity distribution using the suppressed responses;

H(e,s) - joint entropy of odor similarity of both enhanced and suppressed responses;

Entropies were given by:

$H(s) = \sum -p(odor\ similarity)\ log_2(p(odor\ similarity))$

All the distributions were estimated using a normalized histogram and using a bin size of 0.1.

To estimate whether the calculated mutual information was different from chance, we shuffled the odor identities and re-calculated the mutual information (10,000 times).

Shuffled correlation

To calculate shuffled cell similarity, the odor identities of the ORS of each of the two cells were randomly exchanged before calculating the cell similarity. For odor similarity, the cell identities of the population response vector (CRS) of each of the two odors were shuffled before calculating the similarity.

Odor similarity-matching number of mitral cells and tufted cell

To match the number of mitral cells and tufted cells used to construct population vectors, we randomly selected 9 fields of view in the mitral cell layer and 9 fields of view in the EPL containing tufted cells. To match the number of cells in each FOV, we pseudorandomly selected 40 mitral cells and 40 tufted cells. We chose 40 cells because it represented a lower bound of the average number of tufted cells imaged in a given FOV. We used a total set of 528 (odor pairs) X 9 (randomly selected FOVs) X 20 (repeats) and plotted the distribution of odor similarity by performing 20 iterations of randomly selecting 40 mitral and 40 tufted cells across 9 fields of view.

Pharmacology

Animals were implanted with cannulas in the APC using 26 Gauge cannula (Plastics One) at a 50 degree angle from the vertical (Figure S5A) at the same time as the optical window was implanted. Cannulae were implanted bilaterally, but muscimol/saline was injected in only one hemisphere per imaging session. After imaging a given field of view (baseline), muscimol (muscimol hydrobromide, MW=195.01, Sigma) dissolved in cortex buffer (0.5 mg/ml, injecting 1 μl over 5 min) was used to suppress activity in the piriform cortex. No apparent changes in the animals' sniffing, whisking or motor behaviors were observed upon muscimol injection. In a subset of experiments (N=3 mice), we used fluorescent muscimol bodipy (MW=607.46, Life

Science Technologies, 1mg/ml in cortex buffer and 5% DMSO, injected 2µl over 10 min). To account for differences in molecular weight between fluorescent and non-fluorescent muscimol, we injected higher volume of more concentrated drug solution in the fluorescent muscimol experiments. To quantify the spread of the drug, two hours post injection, animals were killed, perfused in PFA, and 100-200 µm sagittal slices were cut and imaged under an epifluorescence microscope. Fluorescent muscimol intensity was assayed at the injection site by calculating the mean fluorescence within a 200 x 200 µm ROI, centered at the site of the cannula tip and used as 'reference'. Across all imaged slices, same size ROIs were selected, centered at the site of highest fluorescence within each slice, and the calculated average fluorescence value normalized by the 'reference'. For control experiments (saline controls), only cortex buffer was used.

For experiments comparing feedback odor responses between awake and anesthetized conditions, a field of view was initially imaged while the animal was awake. The animal was then injected intraperitonealy with ketamine/xylazine (KX, 35/3.5 mg/kg) and lightly anesthetized, preserving strong pedal withdrawal reflex. We waited for 10 minutes after injection before continuing imaging in the same field of view. Care was taken to identify same feedback boutons in the FOV before and after anesthesia. Body temperature was maintained using a heating pad (FST TR200).

Anterior Piriform Cortex (APC) Electrical Stimulation

Animals were implanted with a guide cannula in the anterior piriform cortex (C315GS-4/SP, 26 G, 9 mm below pedestal, Plastics One, Figure S5A), through which an electrode (A-M Systems stainless steel wire, cat #790900, core diameter = 76.2 µm, coated diameter 139.7 µm) placed within an infusion Internal cannula (C315IS-4/SP, Plastics One) was inserted. A skull screw in the right parietal bone served as ground. The electrode tip was gold plated to an

impedance of <50 kΩ. Current pulses were delivered using an Isolated Pulse Stimulator 2100 (A-M Systems). For experiments described in Figure S4A-C (no muscimol), biphasic cathode-leading current pulses (100μs, <30 μA) were used. We did not observe a startle response in the animal at this level of current. For 'odor' and 'odor + electrical stimulation' experiments, we used a set of 20 odors (Odor Set A, Table S1) and followed same delivery protocols as described above; 'odor' and 'odor+electrical stimulation' trials were presented in a randomly interleaved manner. The current pulses (1, 2, 4, 8 or 16) were delivered either at 50Hz or 100Hz during the air period, or 2s from odor onset. Responsiveness for each ROI-odor pair was assessed based on odor presentation in the absence of electrical stimulation.

For experiments described in Figure S5G-K, activity in the APC was suppressed by injecting muscimol dissolved in cortex buffer (0.5 mg/ml, injecting 1 μl over 5 min) through an internal cannula. After muscimol injection, the internal cannula was replaced with the stimulating electrode. Given a steep reduction in number of boutons that responded to the electrical stimulation protocol post muscimol injection, current amplitude was increased to 50 μA to trigger detectable fluorescence changes. We used for further stimulation protocols only boutons that showed a significant response to a strong stimulus (100μs pulse train at 100Hz for 1s) duration. For the different protocols used (1, 2, 4, 8, 16 pulses at 50Hz or 100Hz), each stimulation train was presented 12 times, at 15 seconds ITI. To determine significance of responses to different stimulation trains, a 250 ms interval preceding the electrical was compared to a 250 ms interval after the pulse ($p<0.001$, paired t-test, 12 pulses, separated by 15 seconds).

Histology

Animals were perfused intracardially, the brains were preserved in PFA and sliced in the sagittal plane with 50-200 μm sections. Slices were mounted using VECTASHIELD Mounting Medium containing DAPI and imaged using a confocal microscope.

References

Adam, Y., & Mizrahi, A. (2011). Long-term imaging reveals dynamic changes in the neuronal composition of the glomerular layer. *The Journal of neuroscience*, *31*(22), 7967–73. doi:10.1523/JNEUROSCI.0782-11.2011

Tian, L., Hires, S. A., Mao, T., Huber, D., Chiappe, M. E., Chalasani, S. H., Petreanu, L., et al. (2009). Imaging neural activity in worms, flies and mice with improved GCaMP calcium indicators. *Nat Meth*, *6*(12), 875–881. doi:10.1038/nmeth.1398